Available online at www.sciencedirect.com
ScienceDirect
Journal of Power Sources 159 (2006) 420–430
JOURNAL OF POWER SOURCES
www.elsevier.com/locate/jpowsour

Crystalline phases, morphology and conductivity of PEO:LiTFSI electrolytes in the eutectic region

M. Marzantowicz [a,*], J.R. Dygas [a], F. Krok [a], J.L. Nowiński [a], A. Tomaszewska [b], Z. Florjańczyk [b], E. Zygadło-Monikowska [b]

[a] *Faculty of Physics, Warsaw University of Technology, Koszykowa 75, 00-662 Warszawa, Poland*
[b] *Faculty of Chemistry, Warsaw University of Technology, Noakowskiego 3, 00-664 Warszawa, Poland*

Available online 3 April 2006

Abstract

Polymer electrolytes formed from high molecular weight poly(ethylene oxide) with dissolved $LiN(CF_3SO_2)_2$ salt were obtained by casting from solution. The compositions ranging from 16:1 to 8:1 EO:Li molar ratio were studied by the X-ray diffraction and by impedance spectroscopy simultaneously with polarizing microscope observation. Crystallization processes and the resulting morphology of electrolytes were investigated in the temperature range from 85 to −20 °C in various cooling and heating cycles. For all compositions, coexistence of crystalline phases of pure PEO and PEO_6:LiTFSI complex was found. The results indicate that phase segregation plays a key role in the crystallization process. The amorphous phase acts like a reservoir of salt, which can be injected or drained by crystallizing spherulites of a defined composition. This interaction between pure PEO and PEO_6:LiTFSI complex explains why effective crystallization process leading to a large decrease of conductivity can take place even in compositions close to the eutectic system. In such a system the concentration of salt in remaining amorphous phase can be very different from the initial composition of electrolyte. The ionic conductivity strongly depends on morphology of the electrolyte, which indicates a possibility of achieving high conductivity in the presence of the crystalline phases.

Keywords: Poly(ethylene oxide); LiTFSI; Crystalline phases; Morphology; Ionic conductivity

1. Introduction

Conductivity of electrolytes based on poly(ethylene oxide) (PEO) depends strongly on the presence of crystalline phases, which are usually considered as poorly conductive [1]. The lithium bis(trifluoromethanesulfone)imide salt (LiTFSI) is known to act not only as an ion source, but also as a plasticizer, slowing down the crystallization kinetics by formation of physical cross-linking. Partial phase diagram of the PEO:LiTFSI system was first presented by Vallée et al. in 1992 [2] and then investigated in detail in 1994 [3]. Based on the DSC data, three stoichiometric crystalline compounds with molar ratios 6:1, 3:1 and 2:1 EO monomeric units to Li were reported. Properties of these complexes dominate the region of the phase diagram with the fraction of salt higher than given by the molar ratio 6:1 EO:Li. The crystal structure of the 3:1 complex has been resolved by refinement of the X-ray powder diffraction pattern by Andreev et al. [4,5]. In their model, PEO retains the helical conformation of the chain characteristic for the pure polymer. The cations are located in each turn of the helix. The crystal structures of the other complexes, 6:1 and 2:1 EO:Li, remain unresolved.

The region of the phase diagram between pure PEO and the 6:1 complex was extensively studied due to the presence of the so called "crystallization gap" between 12:1 and 8:1 EO:Li molar ratio [2]. Inhibition of crystallization warrants high conductivity of the system. However, a subsequent study showed that only electrolytes prepared with low molecular weight PEO ($M_w = 4 \times 10^3$ g mol^{-1}) remained amorphous [6]. For high molecular weight PEO ($M_w = 4 \times 10^6$ g mol^{-1}), in the discussed composition range, the crystalline phase of the pure PEO coexists with the 6:1 crystalline complex and the eutectic amorphous phase of molar ratio about 11:1 EO:Li. A similar phase diagram was published by Edman et al. [7]. Based on the diffusion coefficients measured by the pulsed-field-gradient NMR and the DSC data, the mass fractions of the crystalline PEO, the crystalline complex PEO_6:LiTFSI and the disordered eutectic phase of composition given by the molar ratio 9:1 EO:Li were reported for the electrolytes ranging in molar ratio from

* Corresponding author. Tel.: +48 22 6608405; fax: +48 22 6282171.
E-mail address: marzan@mech.pw.edu.pl (M. Marzantowicz).

0378-7753/$ – see front matter © 2006 Elsevier B.V. All rights reserved.
doi:10.1016/j.jpowsour.2006.02.044

100:1 to 8:1 EO:Li [8]. A constant mass fraction equal 0.15 of the disordered phase was postulated for all compositions.

In the debate over the phase composition and the mechanism of ion transport in the "crystallization gap" region, the effect of macro-scale morphology on the properties of the electrolytes has been often underestimated. For the temperature range and cooling rates typical for the investigation of conductivity of polymer electrolytes, the pure PEO crystallizes in a spherulitic morphology [9]. The PEO:LiTFSI complexes of molar ratio 6:1 and 3:1 EO:Li also form spherulites [10,11] and such a morphology is common for complexes of PEO with other salts [12].

In general, crystallization of polymers occurs by regular folding of the macromolecular chain, which forms a layer of specific thickness (lamella). A spherulite can be treated as an aggregate of lamellae, which grows from a nucleation center and fills a spherical volume by more or less regular branching. The morphology of spherulites depends on the conditions of the growth. Depending on the balance between the rate of growth and the rate of perfection of lamellae, different regimes of crystallization take place [13]. Slow crystallization at low overcooling rates leads to the formation of axially oriented, dense structures (regime I), while greater overcooling rates promote fast, dendritic-like growth of the stacks of lamellae (regime III). Between these two limiting cases, spherulites with regular branching of lamellae and perfect spherical shape are formed (regime II). When a regular spherulite is observed between crossed polarizers of an optical microscope the maltese cross pattern can be observed, which signifies perfect alignment of the birefringent crystalline structures [9]. A considerable amount of amorphous phase can be found between the growing lamellae [14]. The thickness of lamellae depends on the molecular weight and on the crystallization temperature. For the high molecular weight PEO, the "long period" (thickness of a lamella and a neighbor amorphous layer) is in the order of ten nanometers as estimated by the small angle X-ray scattering [15,16]. The fraction of the amorphous phase may be reduced in course of the secondary crystallization. An enhancement of conductivity through the crystalline phase forming preferred pathways for ion transport is not likely for such a morphology, as ion transport would occur only at a very short distance along "tunnels" across the lamellae. Therefore, the lamellae may be treated rather like a "detour" than like a "shortcut" for the traveling ions. Enhancement of the conductivity was reported for crystallites grown in oriented way [17], however, in such systems the effect may be due to orientation of the amorphous phase [18].

Since the early investigations of semicrystalline polymer electrolytes it is known, that crystallization may induce phase segregation in non-stoichiometric systems, creating spherulites of different types [12] or regions with varying concentration of salt [19]. The growing lamellae of defined stoichiometry expel non-crystallizable fraction, which can result in a change of the concentration of salt in the surrounding. The rejected material can fill the inter-lamellar spaces only to a small extent and usually it accumulates at the growth front [9]. Such behavior provides a likely explanation for the non-linear growth rate of spherulites in polymer electrolyte [20]. The phase composition of polymer electrolyte is thus complicated. Crystallites of different composition are embedded in the amorphous phase and also contain that phase within the inner structure. We favor the picture that in the multi-phase structure of semicrystalline electrolyte the ionic conductivity relays on percolation of pathways of the phase of high conductivity rather than on the content of various phases [10,21,22]. The continuity of pathways is strongly related to the morphology and depends not on only on the growth of spherulites, but also on the secondary crystallization as has been reported by other authors [23].

In this paper, we focus on the influence on ionic conductivity of the crystallization phenomena and the resulting morphology of electrolyte for the composition range between diluted electrolytes of low salt content in PEO and the PEO_6:LiTFSI complex. This range includes the "crystallization gap" for molar ratio close to 10:1 EO:Li. The results obtained previously by impedance spectroscopy for the PEO:LiTFSI 10:1 electrolyte [24] indicated that a decrease of conductivity by a factor over 100 observed at a constant temperature close to $-10\,^{\circ}C$ can be related to crystallization and development of a multi-phase structure of this electrolyte. Here, with the support of X-ray diffraction and polarizing microscope, which give information on the crystal structure and the microstructure (morphology) of the electrolyte, respectively, we examine why the impact of crystallization upon conductivity may be of a similar magnitude for compositions close to the eutectic and for the compositions corresponding to the stoichiometric crystalline phases: the PEO_6:LiTFSI complex or the pure PEO.

2. Experimental

$LiN(CF_3SO_2)_2$ (Aldrich) was dried under vacuum and added to poly(ethylene oxide) ($M_w = 5 \times 10^6$ g mol^{-1}, Aldrich) in acetonitrile solution. The obtained solution was poured onto a teflon dish and a thin foil was formed after vacuum drying. The average thickness of the obtained foils was about 200 μm. Prior to the measurement, the foils were kept in argon for about 1 month. The results regarding compositions with EO:Li molar ratios equal 16:1, 12:1, 10:1 and 8:1 are presented. A similar procedure was used for obtaining pure PEO, and PEO:LiTFSI of molar ratios 50:1 and 6:1, which serve as a reference.

The X-ray diffraction patterns were obtained on Philips X'Pert diffractometer, with Cu Kα ($\lambda_1 = 1.54056$ Å, $\lambda_2 = 1.54439$ Å) graphite monochromated radiation. The measurement was done in the flat-plate $\theta/2\theta$ geometry on a spinner stage. The rotation period of the spinner was set to 4 s. Discs cut from the electrolyte foils were placed in a gas-tight holder to prevent absorption of water. The cross-section of the holder is shown in Fig. 1a. The cylindrical corpus and cover of the holder were made of brass. The samples (diameter 16 mm) were placed on a stainless steel plate. The vertical position of the plate was adjusted to obtain the correct geometry for the X-ray measurement. Underneath the plate, a small amount of silica gel was placed as moisture absorber and indicator. After placement of the sample, the container was covered with an aluminum foil (thickness about 10 μm), which was pressed to an o-ring by a cover with a round hole over the sample. The base and cover were tightly screwed together. The pressure of argon trapped inside

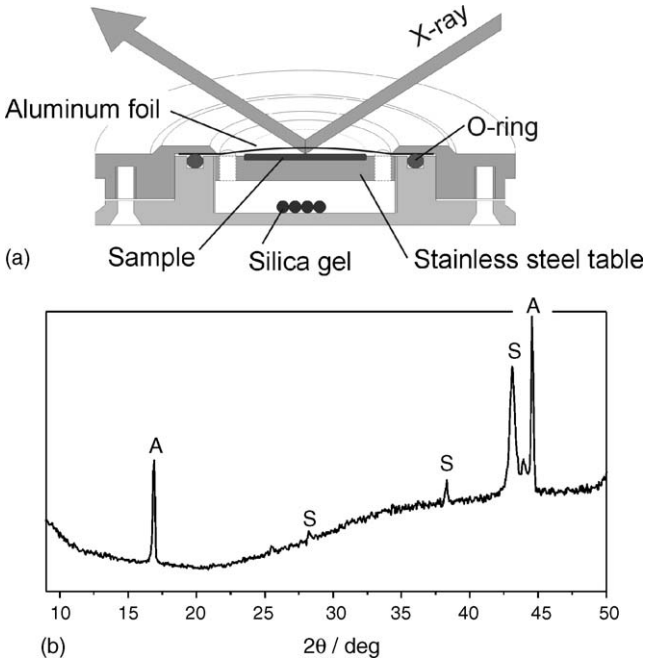

Fig. 1. (a) Scheme cross-section of the sample holder for the X-ray diffraction. (b) The X-ray diffraction pattern of the empty holder. Letter A marks diffraction peaks from the aluminum foil, letter S marks diffraction peaks from the stainless steel table.

the holder gently pushed the aluminum foil upwards, forming a convex dome.

The X-ray diffraction pattern of an empty holder is presented in Fig. 1b. The sharp peaks at about 17° and 44.5° (2θ) are attributed to the aluminum foil. During measurements of polymer samples, the exact position and intensity of these peaks depended strongly on the shape of the aluminum foil, which was not exactly in focus of the X-ray diffractometer. The peaks at ca. 26°, 28.5°, 38.5° and the double peak at 43° (2θ) are attributed to the stainless steel plate.

The polarizing microscope photographs and impedance measurements were taken simultaneously in a custom designed experimental set-up. Glass plates covered with a conductive ITO (indium tin oxide) layer formed a measurement cell, which was placed in a gas-tight holder. The holder was mounted on a microscope stage heated or cooled by Peltier elements in the temperature range from −25 to 115 °C. To prevent moisture condensation on the holder and the microscope objective, the microscope was placed in a dry box. The technical details regarding the set-up have been previously described [21].

Impedance drift detection was an important feature of the measurement program [25]. Detection of changes of the impedance occurring with time is very useful for investigation of phenomena related to phase transitions [10,21,24]. Before and after the acquisition of the whole impedance spectrum, a short test scan was executed, with a wide frequency range from 10^7 to 3.16 Hz and only two frequencies per decade. Basing on the root-mean-square relative difference of the impedance (drift) calculated for these two tests scans, the custom written measurement program modified the temperature ramps. A constant temperature was held as long as the impedance drift was larger than a preset drift limit. This way the mode of experiment was automatically switched between the study of the temperature dependence to the recording of the time dependence at constant temperature of both the microscopic picture and the impedance spectrum. Thus, crystallization and melting of polymer electrolytes could be investigated in semi-isothermal conditions until the system reached steady state. Suitably adjusted drift detection criterion allowed separation of subsequent processes, which otherwise would overlap in the investigated temperature range.

3. Results and discussion

3.1. Electrolytes with excess of the crystalline PEO (16:1 and 12:1 EO:Li molar ratio)

The X-ray diffraction patterns of electrolyte foils as cast from solution are presented in Fig. 2. Data obtained for pure PEO, PEO:LiTFSI 50:1 and 6:1 are also given in Fig. 2 as reference. For the pure PEO and PEO:LiTFSI 50:1, only the semicrystalline PEO was observed. The characteristic peaks, marked with circles in Fig. 2, particularly the two most distinctive: a single peak at 19.1° 2θ and a triple peak at about 23.3° (2θ), are in good agreement with the results obtained by other authors for pure PEO [15,26–28] as well as for diluted PEO-based electrolytes [19,29]. For compositions with higher concentration of salt, the intensity of peaks related to pure PEO was smaller than in pure PEO. Beginning from the 16:1 EO:Li molar ratio, the peaks related to the PEO_6:LiTFSI complex were observed, most characteristic at 11.3°, 14.6° and 22.7° (2θ). For the molar ratio 12:1 EO:Li, the first and the second peak had rather unexpected proportions of intensity, which can be attributed to an effect of preferred orientation not suppressed by spinning. Such an effect was observed only for the sample as cast from solution and can be therefore caused by ordering induced by the preparation procedure. Despite this anomaly, the overall intensity proportions of peaks related to pure PEO and to the PEO_6:LiTFSI complex indicate that the 6:1 crystalline phase constitutes a significant mass fraction of these electrolytes.

The temperature dependence of conductivity calculated from the impedance spectra of the 16:1 and 12:1 compositions is presented in Fig. 3. The samples were initially fused at 80 °C, then measurements were made during cooling down to about −20 °C and then during heating to 80 °C. The impedance drift detection procedure was applied with the drift limit of 2% per hour. Two crystallization events were observed during cooling for both systems, each leading to a decrease of the conductivity. The first process observed above the room temperature caused only a minor decrease of conductivity. The second process that occurred below room temperature had a much stronger effect on conductivity. The observed effects can be understood when the impedance spectra are compared with simultaneously taken photographs from polarizing microscope, Fig. 4. Since similar processes were observed for both compositions, only the results obtained for the 16:1 composition are presented in detail.

In the case of PEO:LITFSI 16:1 electrolyte, the first nucleation seeds became visible about 0.4 h after stepwise cooling to 40 °C. After 0.6 h, coarse-grained spherulites characteristic for

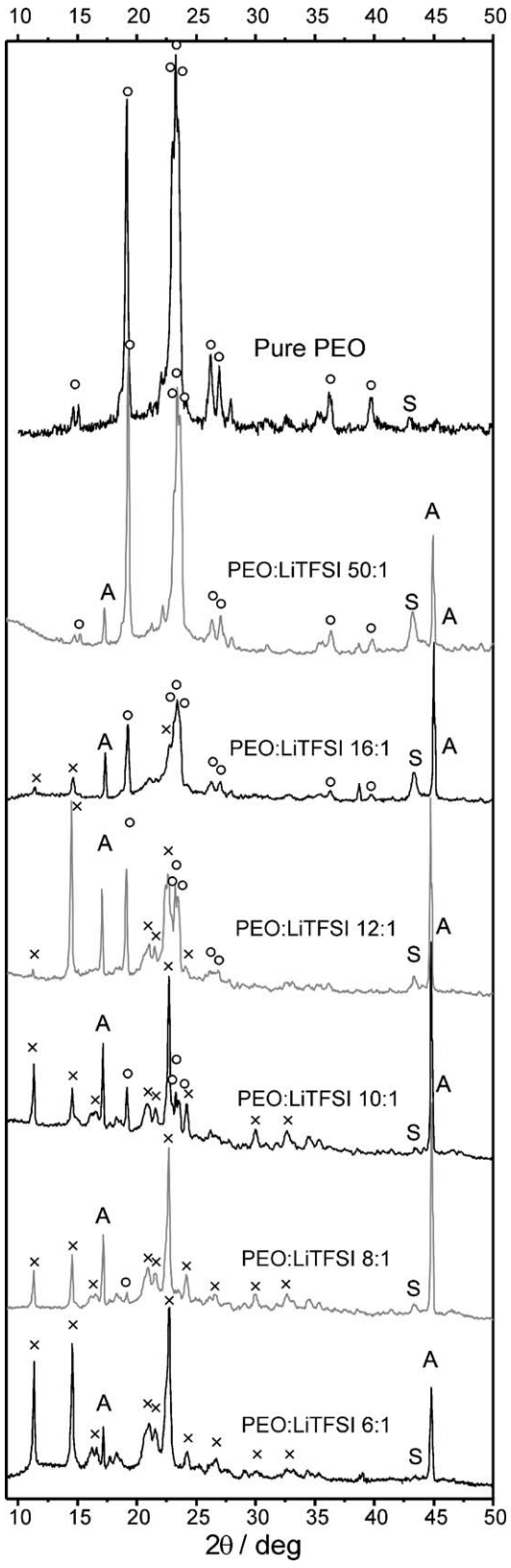

Fig. 2. X-ray diffraction patterns of the PEO:LiTFSI samples "as cast". Patterns of the pure PEO, the diluted electrolyte PEO:LiTFSI 50:1 and the 6:1 complex are given as reference. The main diffraction peaks related to the pure PEO are marked with circles and those related to the 6:1 complex with crosses. Letters A and S mark peaks from aluminum and steel, respectively. The X-ray pattern of the PEO was measured without aluminum foil.

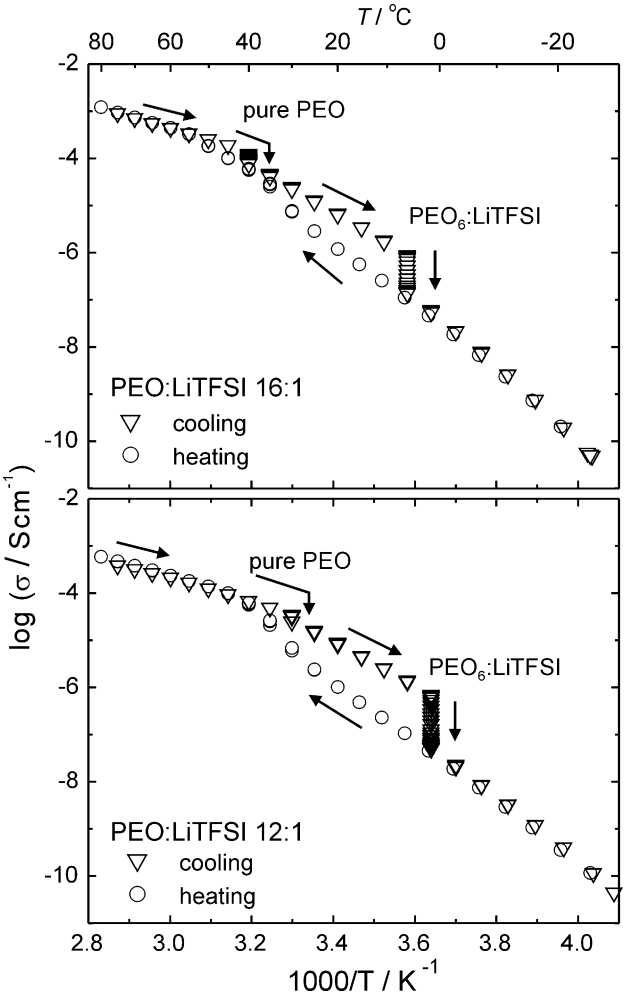

Fig. 3. Temperature dependence of conductivity for PEO:LITFSI 16:1 and 12:1 electrolytes. Isothermal crystallizations of various phases are represented by series of points measured at constant temperature. Vertical arrows indicate the decrease of conductivity with time.

the pure PEO were clearly seen, Fig. 4a. Initially, the growth rate of spherulites was similar to that in pure PEO. However, the growth rate slowed down as the crystallization proceeded and eventually the spherulites ceased to grow. The resulting structure comprised amorphous passes between spherulites, visible as dark areas in Fig. 4b taken after stepwise cooling to 25 °C. An independent experiment, performed on a sample subjected to an analogous temperature treatment, proved that the obtained semicrystalline electrolyte was quite stable at room temperature. The conductivity decreased only by 2% during 3 weeks of conditioning at room temperature. In the case of the 12:1 EO:Li electrolyte, the crystallization occurred in similar way, but the onset of the process was shifted from 40 to 35 °C. Spherulites grown in the 12:1 electrolyte were slightly smaller and the area of amorphous passes was larger than in the case of the 16:1 electrolyte.

The initial fast growth of spherulites, which later slowed down, can be understood when two competing processes are considered: (i) nucleation of chains onto the face of lamella and (ii) change of salt concentration. The temperature at which crystallization of PEO was observed in the PEO:LiTFSI 16:1

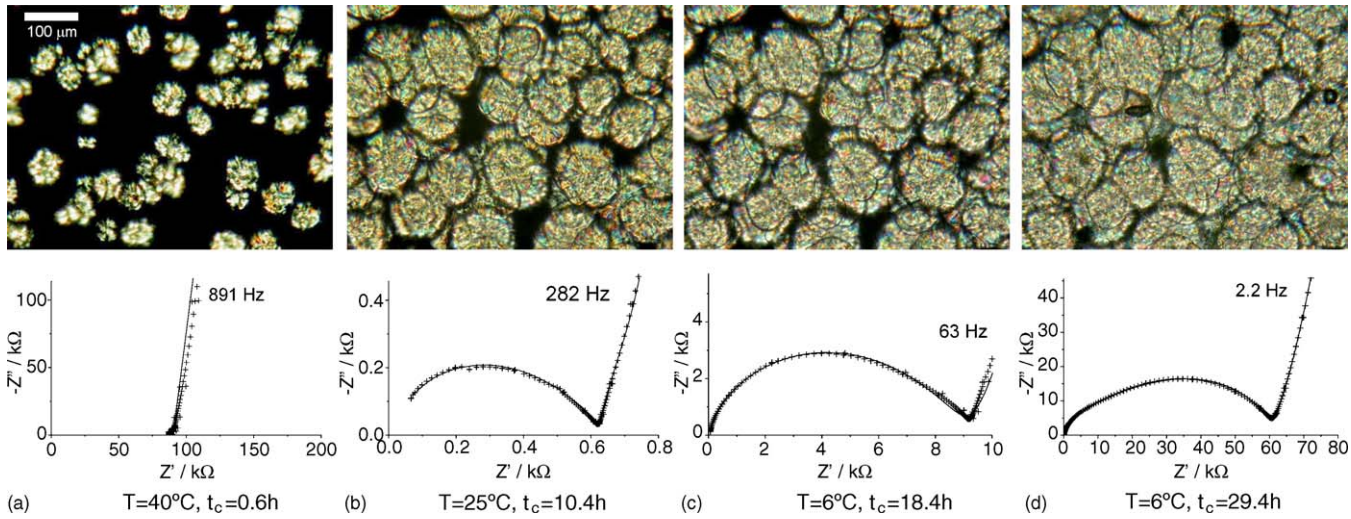

Fig. 4. Polarizing microscope photographs and corresponding complex impedance diagrams recorded during the crystallization of PEO:LiTFSI 16:1 electrolyte. The actual temperature and time counted from cooling to 40 °C are indicated.

electrolyte was 15 °C lower than the crystallization temperature observed for the pure PEO subjected to a similar cooling rate and drift detection [10,24]. Deeper overcooling is needed to overcome the plasticizing effect of LiTFSI salt during the initial growth. Slowing down of the growth rate is caused by the accumulation of the non-crystallizable fraction at the growth front. Conditions for folding of chains at the face of the lamella become less favorable due to the increased concentration of the salt eliminated from the growing PEO spherulite. At a certain point, the gradient of concentration of the salt between the lamella and its surroundings is too high and further growth ceases. Such a process is related to the shift of composition of the remaining amorphous phase towards the liquidus curve on the phase diagram [30].

On cooling of the PEO:LITFSI 16:1 electrolyte below room temperature, a second crystallization event was observed at 6 °C. The total decrease of conductivity was by a factor equal 8 compared as to the factor equal 1.5 during crystallization at 40 °C. In the microscope picture gradual closing of the amorphous passes was observed, proceeding from the spherulite boundary to the center of the pass. Finally, only a few small dark spots remained, which cannot be identified as the amorphous phase but are probably small bubbles of gas trapped at the surface of glass plates, Fig. 4d. For the 12:1 electrolyte, similar changes of the microscope picture and impedance spectra were observed during the second crystallization that took place at 1.5 °C.

It should be noted that the decrease of conductivity was accompanied by the change of shape of the complex plane plot of impedance. The impedance diagram changed from one distorted semicircle to two semicircles, from which two different values of resistance could be estimated by fitting an equivalent circuit. It has been previously demonstrated that such shape of the impedance spectrum is related to the existence of a dense crystalline phase, which creates a very tortuous path for the charge carriers. This "blocking" effect was observed for the pure PEO and for the PEO:LiTFSI 6:1 semicrystalline electrolytes, thus can also be expected for a mixture of both phases [21,22,24].

According to the phase segregation mechanism, it is reasonable to expect that the second crystallization involved the PEO_6:LiTFSI crystalline complex, because the concentration of salt in the amorphous phase between existing PEO spherulites was much higher than that given by the average composition of the electrolyte. In order to confirm such reasoning the X-ray diffraction was performed for the sample that underwent similar treatment. The polymer electrolytes were melted at 80 °C and then cooled down to 25 °C to induce the crystallization of PEO-rich spherulites. In the X-ray diffraction patterns collected a few hours after cooling, only diffraction peaks corresponding to the pure PEO were seen, Fig. 5a. The X-ray patterns of the PEO:LiTFSI 16:1 electrolyte collected 3 h and 8 h after cooling were nearly identical, which confirms that the crystallization process occurred quite rapidly and then ceased. For the 12:1 electrolyte, which was subjected to the same treatment, the intensity of diffraction peaks was considerably lower, and the crystallization process of the pure PEO seemed to be still progressing after 3.7 h.

In order to induce the crystallization at low temperature, the samples were placed in a freezer at −15 °C to promote nucleation and then conditioned for 8 h in a refrigerator at 5 °C. In the diffraction pattern shown in Fig. 5b, the characteristic peaks of the PEO_6:LiTFSI complex appeared in addition to the previously observed peaks related to PEO. For the 12:1 composition the intensity of peaks related to both phases was similar as for the 16:1 electrolyte. The X-ray diffraction patterns collected in the course of the special treatment proved, that the phase, which crystallized in between existing PEO spherulites, consisted mainly of the PEO_6:LiTFSI complex. It is also possible that an inter-growth of the 6:1 phase took place in between the lamellae of the pure PEO. The resulting morphology of the semicrystalline electrolyte was also examined in SEM pictures of the surface of the electrolyte, Fig. 6. For the 16:1 composition, "rough" spherulites consisting mainly of PEO were seen embedded in "smooth" regions rich in the 6:1 phase.

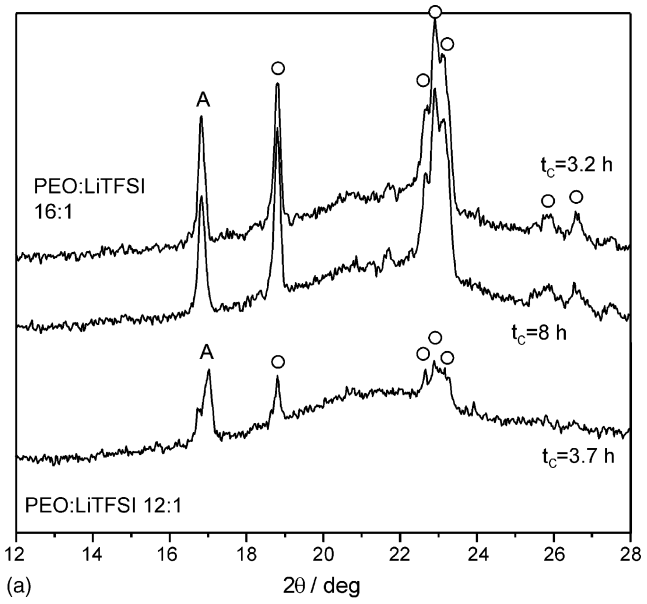

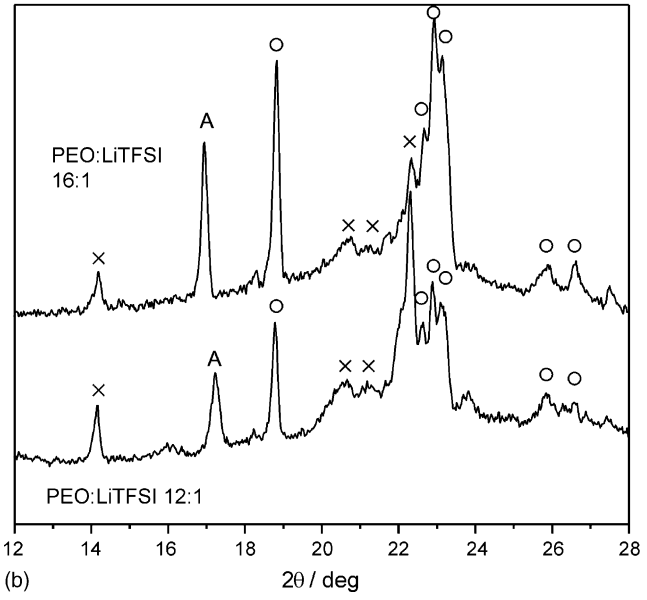

Fig. 5. X-ray diffraction patterns of the PEO:LiTFSI 16:1 and 12:1 electrolytes: (a) after melting the sample at 80 °C and cooling down to room temperature, time of conditioning at room temperature is given; (b) after subsequent freezing to −15 °C and conditioning at 5 °C for 8 h. Diffraction peaks related to the pure PEO and the PEO_6:LiTFSI complex are marked with circles and crosses, respectively. Letter A denotes peak from aluminum foil.

The observed separation of two crystallization processes and the resulting multi-phase morphology is in agreement with the calorimetric results presented by Edman and Doeff [31]. Double endothermic peaks observed by these authors for the PEO:LiTFSI samples, which had been stored below room temperature after melting, could result from such a morphology. Our observations corresponded well with the phase segregation and with the assumption that domains of the PEO_6:LiTFSI complex existed at temperature slightly higher than the melting point [8]. However, in contrast to what was stated be Edman et al. [8,31], in the electrolytes with a higher content of PEO than the eutectic composition, the formation of nucleation seeds seemed to be the

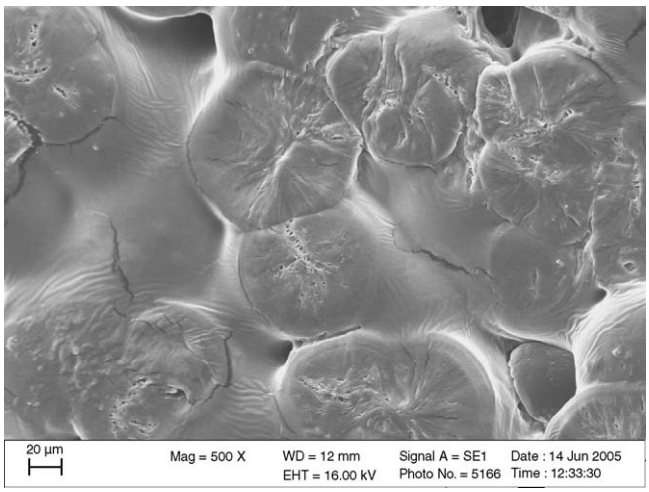

Fig. 6. Scanning electron microscope image of the surface of the semicrystalline PEO:LiTFSI 16:1 electrolyte.

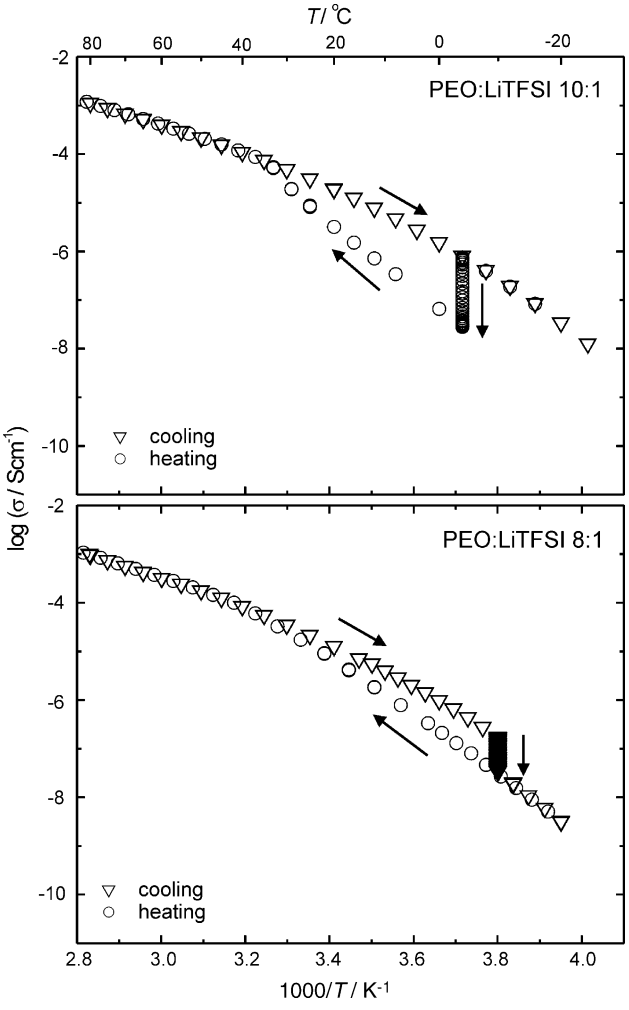

Fig. 7. Temperature dependence of the conductivity for the PEO:LITFSI of molar ratio 10:1 and 8:1 EO:Li. Isothermal crystallization is represented by a series of points measured at a constant temperature. Vertical arrows indicate the decrease of conductivity with time.

rate limiting factor only for crystallization of the PEO_6:LiTFSI complex but not for the pure PEO. Completion of the crystallization process was dependent on the interaction between the two crystalline phases. It is worth noting, that the crystallization of PEO caused only a minor decrease of conductivity, while the crystallization of PEO_6:LiTFSI complex was responsible for the blocking of the conductivity pathways. If the latter process was prevented, a semicrystalline system with a relatively high ionic conductivity could be obtained.

3.2. Electrolytes with excess of the 6:1 PEO:LiTFSI complex (10:1 and 8:1 EO:Li molar ratio)

In the case of electrolytes of molar ratios 10:1 and 8:1 EO:Li, the intensity of the X-ray diffraction peaks related to the pure PEO is smaller than the intensity of the reflexes due to the PEO_6:LiTFSI phase, Fig. 2. For the PEO:LiTFSI 8:1 composition, only one of the characteristic peaks related to PEO could be clearly distinguished. When diffraction patterns of the 10:1

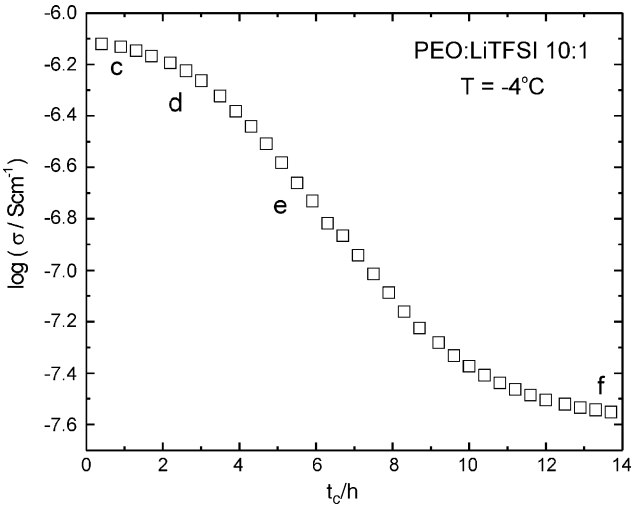

Fig. 8. Time dependence of the conductivity of the PEO:LITFSI 10:1 electrolyte during the crystallization at −4 °C (compare Fig. 7). Letters (c–f) correspond to photographs in Fig. 9.

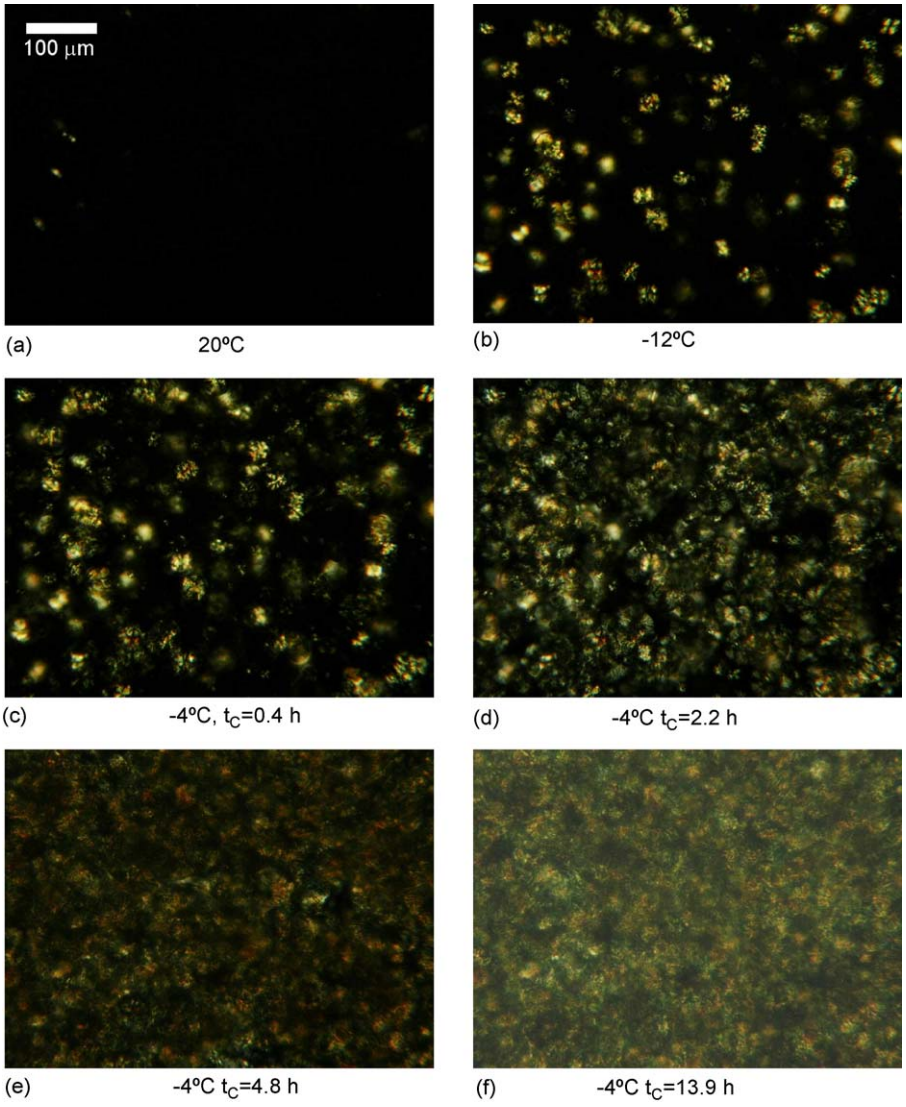

Fig. 9. Polarizing microscope photographs of the PEO:LiTFSI 10:1 electrolyte taken on cooling and subsequent heating simultaneously to impedance measurement. The actual temperature and the time counted from heating to −4 °C are indicated. Letters (c–f) correspond to points marked in Fig. 8. Brightness was enhanced in photograph (f) to visualize the structure.

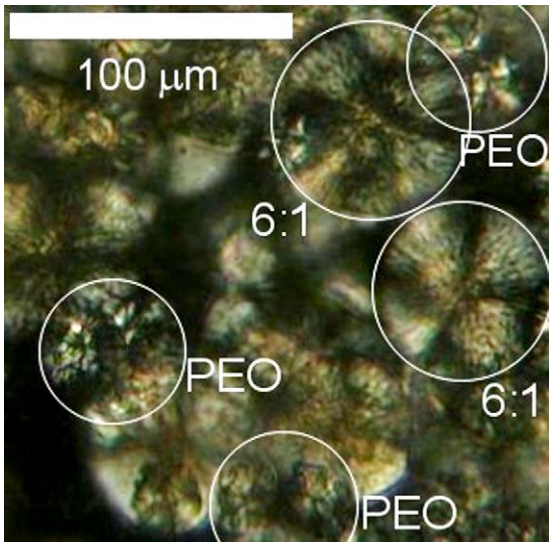

Fig. 10. Spherulites typical for the pure PEO and for the PEO_6:LiTFSI complex observed at −4 °C during crystallization on heating of the rapidly cooled PEO:LiTFSI 10:1 electrolyte.

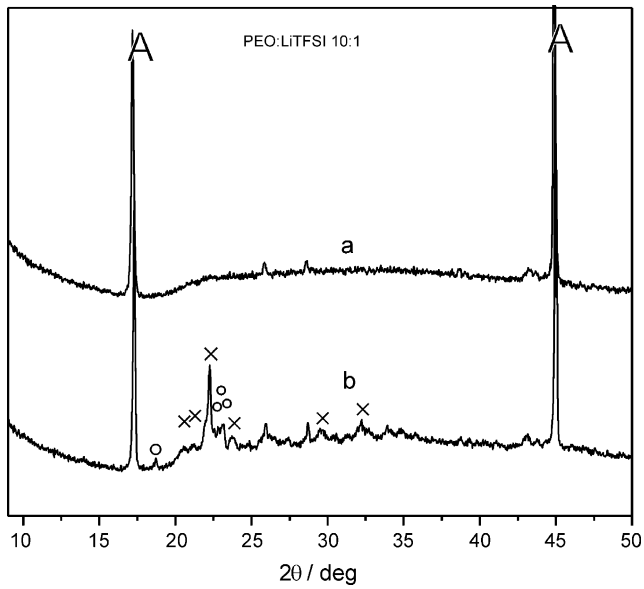

Fig. 11. X-ray diffraction patterns measured at room temperature for (a) the amorphous PEO:LiTFSI 10:1 electrolyte 2 h after melting; (b) the semicrystalline PEO:LiTFSI 10:1 electrolyte after freezing the sample to −15 °C and conditioning at 5 °C (b). Diffraction peaks related to the pure PEO and the PEO_6:LiTFSI complex were marked with circles and crosses, respectively. Letter A denotes peaks from aluminum foil.

and 8:1 electrolytes are compared with that of the stoichiometric PEO:LiTFSI 6:1 electrolyte, it is concluded that the amount of the crystalline 6:1 phase in all three samples is of the same order of magnitude. However, because of differences in the thickness of the samples and absorption of X-rays by the aluminum foil, this can be treated only as a rough estimation. No attempt was made to compute the mass fraction of various phases in each composition.

In contrast to the electrolytes of lower salt content, for the electrolytes of 10:1 and 8:1 molar ratio there is no indication for a process that would lead to a noticeable decrease of conductivity at temperatures above 0 °C during cooling of the molten electrolyte, Fig. 7. Below 0 °C a slightly different behavior was observed for each of the samples. For the PEO:LiTFSI 10:1 electrolyte, on cooling to −20 °C the conductivity followed the Vogel–Tamman–Fulcher relationship. A significant decrease of conductivity was detected on subsequent heating at −4 °C, Fig. 8. For the 8:1 EO:Li electrolyte a less pronounced decrease of conductivity was observed on cooling at −10 °C.

From the observed dependence of conductivity on temperature one could expect that in the PEO:LiTFSI 10:1 electrolyte no crystallization process took place on cooling and only during the subsequent heating nucleation seeds necessary for crystallization were formed. However, polarizing microscope pictures revealed a more complex behavior. The first small spherulites could be seen on cooling at 20 °C, Fig. 9a. The appearance of small crystallites did not cause a noticeable drift of impedance, so the crystallization was not detected and the data acquisition program proceeded with measurements at lower temperatures. A slow growth of spherulites with a decreasing rate

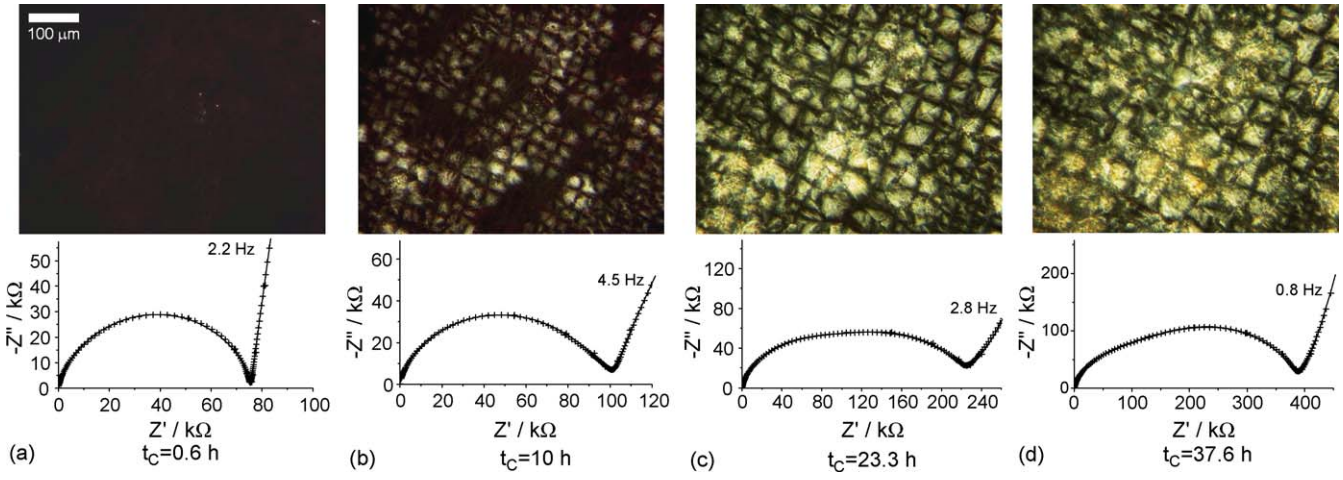

Fig. 12. Polarizing microscope photographs and corresponding complex impedance diagrams recorded during the crystallization at −10 °C of the PEO:LiTFSI 8:1 electrolyte (compare Fig. 7). The time counted from cooling to −10 °C is indicated.

was observed during stepwise cooling down to −12 °C. Below −12 °C the growth ceased, Fig. 9b. Judging from their coarse-grained shape and lack of the maltese cross, the majority of observed spherulites could be ascribed to the pure PEO. On subsequent heating, a large number of new nucleation seeds was observed at −4 °C. The growing spherulites were identified as belonging mainly to the PEO_6:LiTFSI complex since they exhibited a weak maltese cross pattern and circular shape. However, as the crystallization at −4 °C continued, new spherulites characteristic for pure PEO also appeared and the already present PEO spherulites increased in size, Fig. 9d. In consequence, after about 5 h at −4 °C, the entire visible area was filled with spherulites of both types, Fig. 9e. Further inter-penetration and densification of the crystallites resulted in minor changes of the microscope picture, but caused a very pronounced decrease of the conductivity, Fig. 8 and Fig. 9e–f.

The observed development of the semicrystalline morphology indicates that there is a strong interaction between the two crystallizing phases: the pure PEO and the PEO_6:LiTFSI complex. The amorphous phase acts as a reservoir of salt, which can be rejected from or incorporated into the crystalline structures. The crystallization process induces phase segregation and division of the electrolyte into regions with excess of one of the crystalline phases. Such a picture seems to be in good agreement with the "domain" model proposed by Edman et al. [8]. In order to confirm that such an interaction also takes place in a system devoid of the PEO nucleation seeds, an additional experiment was performed. The molten 10:1 EO:Li electrolyte was rapidly cooled to −20 °C and then temperature was gradually increased. Crystallization was detected by the impedance drift at the same temperature of −4 °C and caused a similar decrease of conductivity. In the polarizing microscope pictures, simul-

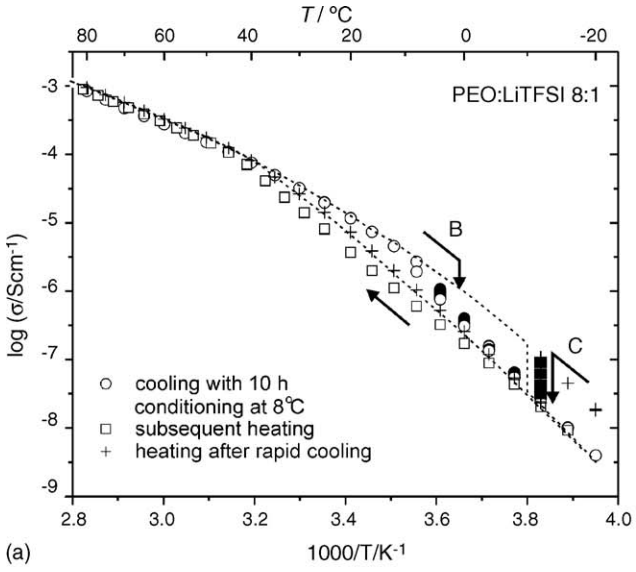

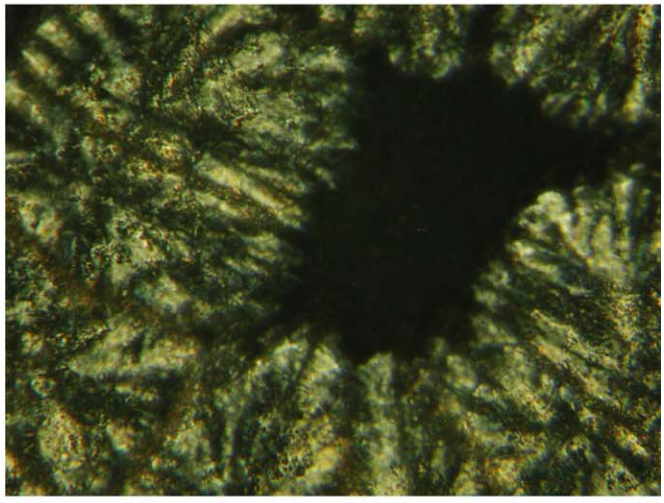

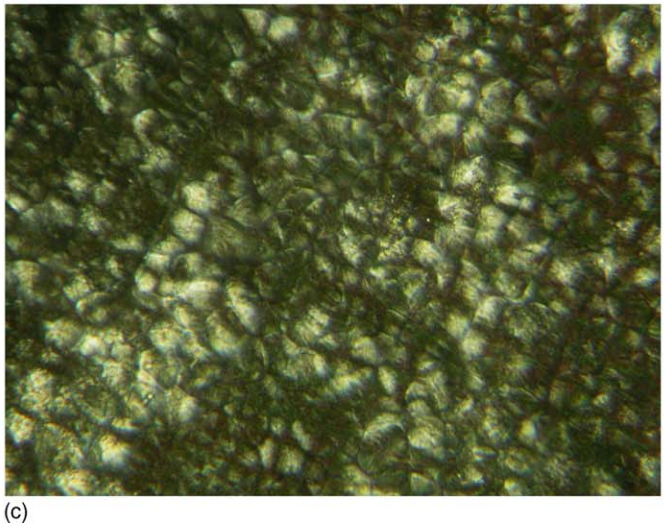

Fig. 13. (a) Conductivity of the PEO:LiTFSI 8:1 electrolyte during different thermal runs. Letters B and C mark the crystallization processes leading to the different morphologies: (b) axialitic at −12 °C after the crystallization initiated during conditioning at 8 °C and gradual cooling or (c) spherulitic at −12 °C after crystallization at that temperature on heating after rapid cooling.

taneous nucleation and growth of the two types of spherulites was observed (Fig. 10). Although in the resulting microstructure the spherulites of the PEO_6:LiTFSI complex filled a majority of the visible area, it seemed that the growth of pure PEO spherulites in their proximity was necessary for the development of the 6:1 crystalline phase. Peaks corresponding to the both phases were also observed in the X-ray diffraction pattern of the PEO:LiTFSI 10:1 sample quenched to −15 °C and conditioned at 5 °C, Fig. 11. Apparently, the rapid cooling resulted in the formation of nucleation seeds and initial segregation of both phases, which allowed an effective crystallization process at low temperature.

The microscope pictures and corresponding complex impedance diagrams obtained during crystallization of the PEO:LiTFSI 8:1 electrolyte, which took place at −10 °C on cooling are shown in Fig. 12. Initially, only spherulites corresponding to the 6:1 EO:Li complex were observed, Fig. 12b. However, as the observed area became filled with spherulites, some brighter areas were observed, exhibiting a granular pattern, Fig. 12c and d. Development of these secondary structures was accompanied by a decrease of conductivity. Significant changes in the shape of complex plane plot of impedance were observed, Fig. 12. Occurrence of two semicircles clearly indicates blocking of ion transport by the crystalline phase, as described above for the 16:1 electrolyte. Such a course of crystallization seems to be similar to the inter-penetration observed in blends of different polymers, which occurs when enough amorphous phase is present in between the lamellae of the existing structure, so that the lamellae of the secondary compound can develop in those areas [32]. Similar conditions may be present in the microstructure of the PEO:LiTFSI 8:1 formed during the initial stage of crystallization, Fig. 12b. Since the amorphous phase between the lamellae of the PEO_6:LiTFSI complex is expected to have concentration of salt lower than that corresponding to the average composition, growth of the PEO crystallites may proceed, competing with the expected secondary crystallization process of the 6:1 complex [9].

The described morphology, obtained by crystallization on cooling, is not the only one possible for the PEO:LiTFSI 8:1 electrolyte. When cooling of molten electrolyte was interrupted at 8 °C and the sample was kept at that temperature for 10 h, an axialitic morphology was obtained instead of the spherulitic one, Fig. 13b. The growth process proceeded gradually on decrease of temperature. Surprisingly, between the crystallites amorphous areas remained even after further cooling down to −20 °C and subsequent heating. Despite differences in the microstructure, the values of ionic conductivity for axialitic and spherulitic morphologies are comparable. Another interesting feature of the axialitic morphology is the higher melting temperature, observed in the temperature dependence of conductivity, Fig. 13a, and also in the microscope observations. The most likely explanation is that the lamellae are wider and more perfect for the axialitic crystallites, as is expected for structures developed in crystallization regime I. Transport of ions within such a microstructure would be heavily constrained, therefore restricting available conduction paths to amorphous areas outside boundaries of the axialites. Higher melting temperature may result from wide lamellae formed by crystallization in regime I or intermediate regime I/II, while the crystallites grown after deep quenching (regime II/III) may contain more amorphous phase in between coarse-shaped thin lamellae and therefore exhibit a lower melting temperature.

4. Conclusions

Two types of spherulites have been identified in the polarizing microscope pictures of the PEO:LITFSI electrolytes: the coarse-grained spherulites typical for pure PEO and the regular shaped spherulites with the maltese cross pattern typical for the PEO_6:LiTFSI complex. In the X-ray diffraction patterns of the studied electrolytes, the peaks related to the pure PEO and to the 6:1 EO:Li complex were identified and used for qualitative phase analysis. In the diffraction pattern of the electrolyte of the molar ratio 6:1 EO:Li, none of the diffraction peaks of PEO was detected, which indicates that the 6:1 electrolyte, obtained by casting from solution, contained only one crystalline phase. However, the quality of the X-ray pattern was not satisfactory for resolving of the crystalline structure of the PEO_6:LiTFSI complex [33], probably due to the influence of the spherulitic morphology.

The crystallization near the eutectic composition involves the interaction of three phases: the crystalline PEO, the crystalline 6:1 EO:Li complex and the amorphous phase. During growth of a spherulite of a certain crystalline phase, the salt is rejected to or drained from the neighboring amorphous region. The local composition of the amorphous phase is thus shifted towards that of the competing crystalline phase and the crystallization of the other phase becomes favorable. During the crystallization a segregation process takes place, resulting in the creation of large crystalline regions, which are rich or poor in salt, rather than the formation of small domains, which could be expected for the eutectic crystallization. The resulting dense crystalline structure strongly blocks ion transport. The interaction between phases explains why the crystallization may proceed quite effectively even for the molar ratio equal about 10:1 EO:Li, for which the "crystallization gap" was claimed based on the observations pertaining to electrolytes based on the low molecular weight PEO.

For compositions far from the eutectic, the phase segregation becomes less effective, so that two independent crystallization processes are observed: the crystallization of the pure PEO occurring above room temperature and the crystallization dominated by the PEO_6:LiTFSI complex below room temperature. As long as the second crystallization process does not take place, the conductivity remains nearly as high as in the case of the amorphous electrolyte.

For certain thermal treatment of the PEO:LiTFSI electrolytes a metastable state was observed, in which growth of the spherulites of one type had ceased, leaving a number of amorphous pathways, which resulted in the morphology favorable for the ionic transport. For the development of a polymer electrolyte suitable for the application in lithium ion batteries this observation opens a perspective of performing a "controlled" crystallization process, aimed at obtaining a stable semicrystalline morphology with amorphous pathways of composition inhibiting further crystallization and warranting high conduc-

tivity. Such an approach may be competitive to the attempts towards a complete inhibition of the crystallization of polyether based polymer electrolytes.

References

[1] C. Berthier, W. Gorecki, M. Miner, M.B. Armand, J.M. Chabagno, P. Rigaud, Solid State Ionics 11 (1983) 91.
[2] A. Vallée, S. Besner, J. Prud'homme, Electrochim. Acta 37 (1992) 1579.
[3] S. Lascaud, M. Perrier, A. Vallée, S. Besner, J. Prud'homme, M. Armand, Macromolecules 27 (1994) 7469.
[4] Y.G. Andreev, P. Lightfoot, P.G. Bruce, J. Appl. Cryst 30 (1997) 294.
[5] Y.G. Andreev, P.G. Bruce, J. Phys. Conden. Matter 13 (2001) 8245.
[6] C. Labreche, I. Lévesque, J. Prud'homme, Macromolecules 29 (1996) 7795.
[7] L. Edman, A. Ferry, M.M. Doeff, J. Mater. Res. 15 (2000) 1950.
[8] L. Edman, A. Ferry, G. Orädd, Phys. Rev. E 65 (2002) 042803.
[9] B. Wunderlich, Macromolecular Physics, Academic Press, New York, 1973.
[10] M. Marzantowicz, J.R. Dygas, F. Krok, A. Molenda, E. Zygadło-Monikowska, Z. Florjańczyk, Mol. Phys. Rep. 35 (2002) 65.
[11] M. Marzantowicz, J.R. Dygas, F. Krok, A. Łasińska, Z. Florjańczyk, E. Zygadło-Monikowska, A. Affek, Electrochim. Acta 50 (2005) 3969.
[12] R. Neat, M. Glasse, R. Linford, A. Hooper, Solid State Ionics 18/19 (1986) 1088.
[13] J.D. Hoffman, R.L. Miller, Polymer 38 (1997) 3151.
[14] J.M. Schultz, M.J. Miles, J. Polym. Sci. B: Polym. Phys. 36 (1998) 2311.
[15] M.S. Lisowski, Q. Liu, J. Cho, J. Runt, F. Yeh, B.S. Hsiao, Macromolecules 33 (2000) 4842.
[16] L.G. Beekmans, D.W. van der Meer, G.J. Vansco, Polymer 43 (2002) 1887.
[17] D. Golodnitsky, E. Livshits, Y. Resenberg, I. Lapides, E. Peled, Solid State Ionics 147 (2002) 265.
[18] O. Dürr, W. Dieterich, P. Maass, A. Nitzan, J. Phys. Chem. B 106 (2002) 6149.
[19] C.D. Robitaille, D. Fateaux, J. Electrochem. Soc. 133 (1986) 315.
[20] B.K. Choi, Solid State Ionics 168 (2004) 123.
[21] M. Marzantowicz, J.R. Dygas, F. Krok, A. Łasińska, Z. Florjańczyk, E. Zygadło-Monikowska, Electrochim. Acta 51 (2006) 1713.
[22] M. Marzantowicz, J.R. Dygas, W. Jenninger, I. Alig, Solid State Ionics 176 (2005) 2115.
[23] B.K. Choi, Y.W. Kim, Electrochim. Acta 49 (2004) 2307.
[24] J.R. Dygas, B. Misztal-Faraj, Z. Florjańczyk, F. Krok, M. Marzantowicz, E. Zygadło-Monikowska, Solid State Ionics 157 (2003) 249.
[25] J.R. Dygas, P. Kurek, M.W. Breiter, Electrochim. Acta 40 (1995) 1545.
[26] D.R. Payne, P.V. Wright, Polymer 23 (1982) 690.
[27] G.B. Appetecchi, W. Henderson, P. Villano, M. Berrettoni, S. Passerini, J. Electrochem. Soc. 148 (2001) A1171.
[28] C.S. Liao, W.B. Ye, Electrochim. Acta 49 (2004) 4993.
[29] W.J. Macklin, R.J. Neat, S.S. Sandhu, Electrochim. Acta 37 (1992) 1715.
[30] A.D. Pelton, in: P. Haasen (Ed.), Phase Transformations in Materials, VCH, Weinheim, 1991, p. 230.
[31] L. Edman, M.M. Doeff, Solid State Ionics 158 (2003) 177.
[32] Y. Nozue, S. Hirano, N. Kawasaki, S. Ueno, N. Yagi, T. Nishi, Y. Amemiya, Polymer 45 (2004) 8593.
[33] Y.G. Andreev, private communication.